Accepted for presentation at the 51st Annual Conference on Information Sciences and Systems, Johns Hopkins University, Whiting School of Engineering's Department of Electrical and Computer Engineering, Baltimore, MD, March 22-24, 2017

On the Improvement of Spectral Efficiency in Mobile Networks: Rate and Mobility Analysis

Zhong Zheng[*] and Zygmunt J. Haas[*◊]

[*] Department of Computer Science, University of Texas at Dallas, Richardson, TX 75080, USA
Email: {zheng.zhong1, haas}@utdallas.edu

[◊] School of Electrical and Computer Engineering, Cornell University, Ithaca, NY 14853, USA
Email: zhaas@cornell.edu

***Abstract*—In this work[1], we consider a mobile distributed MIMO architecture, where the communicating nodes continuously recruit clusters of adjacent transmit and receive nodes to operate as mobile and temporary antenna arrays. As the channel conditions change due to node mobility, the clusters are reconfigured to best serve the communicating nodes. The reconfiguration rate depends on the required system performance, exhibiting a tradeoff between performance and complexity. Our results show that there is an optimal number of transmit nodes (out of the nodes with most favorable channel conditions) to maximize the system achievable rate, which we quantify by closed-form expressions. With the nodes being modeled as Brownian motions, the time interval to reselect a new transmit cluster is obtained analytically and serves to estimate the order of magnitude of the required cluster reselection time for a practical random walk models.**

Keywords—Distributed MIMO; mobile network; random matrix theory; Brownian motion.

I. INTRODUCTION

Recently, Distributed MIMO (D-MIMO) has attracted increasing attention in improving the performance of wireless communications, where individual transceivers are only equipped with small number of antennas. By grouping a number of such transceivers to jointly transmit and/or receive the information symbols, the formed distributed antenna arrays can be used similarly to the traditional multi-antenna transceivers and achieve similar performance as the Co-located MIMO (C-MIMO) ([1]). As the individual transceivers are typically separated by much larger distance compared to the wavelength of the carrier frequency, some of the harmful signal propagation effects in C-MIMO, such as the spatial correlation among antenna elements ([2]), can be circumvented in D-MIMO systems ([3]).

In literature, the D-MIMO has been applied in the stationary infrastructure-based systems, where base stations are pre-arranged in fixed clusters to form distributed antenna arrays. The purposes of such systems, termed Distributed Antenna System (DAS) ([4]) or network MIMO ([5]), are to improve the coverage area and the spectral efficiency of the overall cellular systems, where the users' data streams and the cooperation signaling among base stations are conveyed through the infrastructure networks. Therein, the performance of these systems, such as the ergodic capacity and the outage probability, are evaluated assuming either a particular fixed antenna placement ([6]-[8]) or stochastic antenna placements over a restricted topology, e.g., Wyner's circular model ([9]). These assumptions are relevant in the cellular network scenarios, where the locations of the base stations are either fixed or can be controlled.

The D-MIMO schemes are also called cooperative or virtual MIMO, where the clusters may be formed by small footprint devices and the cooperation signaling is exchanged wirelessly. The formed distributed antenna arrays are spanned over more generic topologies, compared to the infrastructure-based architecture of DAS. Nevertheless, the performance analysis for DAS in [4]-[9] cannot be applied to a more general mobile environments, as is the case of our architecture.

In [10]-[12], the performance of the cooperative MIMO in sensor networks is evaluated in term of the energy efficiency, where the sensor nodes in each cluster are assumed to have the same location. Therefore, the topological impact of the clusters is not investigated. When the clusters are formed by user terminals, the performance evaluations are only conducted via simulations ([13], [14]) or measurement campaigns ([15]).

When the system architecture is mobile and subject to dynamic changes due to the device mobility, timely cluster reconfigurations are required to fully utilize the benefit of the MIMO transmission. The cluster formation algorithms, such as those in [13] and [14], rely on the assumption of slowly-varying channel and thus, are not suitable for mobile networks with relatively fast cluster variations. To the best of our knowledge, the nodes' mobility patterns have not been taken into account in designing the cluster reconfigurations of cooperative distributed MIMO as the network topology changes, and the corresponding computational complexity incurred by the cluster reconfigurations is not known.

To address these issues, we consider a D-MIMO system formed by mobile user devices. The users are randomly distributed and roaming within certain geographical area. The performance of such D-MIMO system is investigated, when a subset of available transmit nodes with most favorable channel conditions is activated to form the transmit cluster. We aim to gain insight into the questions: (1) how many transmit nodes

[1] This work was supported in part by the NSF Grant numbers ECCS-1308208 and ECCS-1533282.

are needed to meet the rate requirement and (2) how often the cluster reconfiguration should be performed due to node mobility. With these distinct features in mind, the considered D-MIMO system is termed in this work as the Reconfigurable Distributed MIMO (RD-MIMO). Using Random Matrix Theory, we address the first question by deriving the closed-form expression of the average achievable rate of the RD-MIMO system, which is the average of ergodic capacity over all possible realizations of node placements. Based on the obtained results, we observe that an optimal number of nodes, typically less than the total number of available nodes, is needed to maximize the achievable rate of RD-MIMO. The second question is answered via the cluster reselection time, after which a new subset of transmit nodes should be recruited due to node mobility. By assuming that the transmit nodes are Brownian particles, the node reselection time is set to capture a given percent of the reconfiguration events, defined by the transmitter selection criterion. The results obtained for the Brownian motion model provide estimates for the order of magnitude of the cluster reselection times in realistic mobile network scenarios and the computational complexity incurred by the reselection scales as $\mathcal{O}(K^2 \log K)$, where K is the number of available transmit nodes.

II. System Model

Consider a wireless communication network with K transmit and N receive nodes, where each transceiver is equipped with two independent radio interfaces, such as cellular and WiFi radios. Among the transmit/receive nodes, there exists a head node that initiates/terminates a user's data stream. Other neighboring transmit/receive nodes are assisting nodes and can communicate with the head node via the local high-speed WiFi links. The K transmit nodes form a cooperative transmit cluster, while the head node is responsible for encoding the information symbols into transmit signals, for distributing the encoded signals to the corresponding assisting nodes, and for synchronizing the cellular radio transmissions from the transmit nodes to the receive nodes. Similarly, the N receive nodes form a cooperative receive cluster, while the receive head node collects the received signals from its assisting nodes and decodes the receive symbols. In this work, we assume the node cooperation within each cluster is performed over the reliable and high-speed WiFi networks, and the transmit and receive clusters operate as distributed antenna arrays. The cellular transmission between clusters is the bottleneck of the RD-MIMO system. This assumption is reasonable since the rate of the local WiFi transmission is much higher than the cellular transmission between distant clusters.

A. Signal Model

Given a transmit vector[2] $\mathbf{x}(t) = [x_1(t), \dots, x_K(t)]^{\mathrm{T}}$, where $x_k(t)$ denotes the transmit signal of node k at time t, the receive vector $\mathbf{y}(t) = [y_1(t), \dots, y_N(t)]^{\mathrm{T}}$ is written as

$$\mathbf{y}(t) = (\mathbf{G}(t) \circ \mathbf{H}(t))\mathbf{x}(t) + \mathbf{n}(t), \quad (1)$$

where $y_n(t)$ is the received signal of node n at time t, the operation $\circ$ denotes the entry-wise matrix multiplication, and $\mathbf{H}(t)$ is an $N \times K$ matrix representing the fast fading coefficients between the transmit and the receive clusters. We assume the entries of $\mathbf{H}(t)$ are *i.i.d.* standard complex Gaussian distributed. Letting T_c be the channel coherence time and $M \cdot T_c$ the length of each coding block, the channel $\mathbf{H}(t)$ remains constant over each coherence period and is *i.i.d.* across different coherence periods. The distance-dependent path losses are modeled as matrix $\mathbf{G}(t)$, with the entry $g_{n,k}(t)$ denoting the square root of the average channel gain between the k^{th} transmit node and the n^{th} receive node, such that

$$g_{n,k}(t) = c_p \, d_{n,k}(t)^{-\alpha/2}, \quad (2)$$

where c_p depends on the carrier frequency, α (≥ 2) is the path loss exponent, and $d_{n,k}(t)$ is the distance between the k^{th} transmit node and the n^{th} receive node. The additive noise $\mathbf{n}(t)$ is modeled as *i.i.d.* complex Gaussian vector with power ρ^2, i.e., $\mathbf{n}(t) \sim \mathcal{CN}(\mathbf{0}, \rho^2\mathbf{I})$. In this work, we have adopted the following assumptions about the signal model:

(A1) Within each cluster, the head node performs joint encoding/decoding of the transmit/receive signals. With relatively low node mobility, the path loss $\mathbf{G}(t)$ varies slowly over the duration of multiple coding blocks. For each block interval $M \cdot T_c$, $\mathbf{G}(t)$ is treated as a constant matrix, and the fast fading $\mathbf{H}(t)$ is ergodic.

(A2) In both the transmit and receive clusters, the signals are perfectly exchanged between the head node and the assisting nodes. Instantaneous CSIs are available at the receive nodes.

(A3) At the transmit nodes, the transmit symbol $\mathbf{x}(t)$ is Gaussian distributed with the covariance matrix[3] $\mathbb{E}[\mathbf{x}(t)\mathbf{x}(t)^{\dagger}] = \mathbf{Q}$, i.e., $\mathbf{x}(t) \sim \mathcal{CN}(\mathbf{0}, \mathbf{Q})$.

In particular, we consider the case when the transmit and the receive clusters are spanned over planar squares as shown in Fig. 1. The distance between the closest edges of the two clusters is denoted as d, with the receive cluster located at the origin O. The transmit nodes are randomly distributed in the square area $\mathcal{U}$, where the edge length of $\mathcal{U}$ is denoted as s. To obtain tractable analysis and gain insight into the impacts of the distributed transmit nodes, we assume that the distance d is much larger than the dimension of the receive cluster. In this setting, the average channel gain is approximated as

$$g_{n,k}(t)^2 \approx g_k(t)^2, \quad 1 \leq n \leq N \text{ and } 1 \leq k \leq K. \quad (3)$$

The assumption of square clusters allows tractable analysis for the achievable rate and for the cluster reselection time of the RD-MIMO system. Performance analysis and comparisons with other cluster models are left for future works.

B. Node Mobility Model

Denote the locations of the transmit nodes at time t as $a_1(t), \dots, a_K(t)$, where $0 \leq t \leq t_{\max}$, and $t_{\max}$ is the stopping time. The location of the i^{th} transmit node is represented as a complex number $a_i(t) = p_i(t) + \mathrm{i}\, q_i(t)$, where $p_i(t)$ and $q_i(t)$ are horizontal and vertical coordinates on the Euclidean

[2] $(\cdot)^{\mathrm{T}}$ denotes the transpose operation.

[3] $(\cdot)^{\dagger}$ denotes complex conjugate and transpose operation.

plane in Fig. 1, respectively. We model a node motion along the two coordinates as independent Brownian motions with reflected boundaries as described below. We consider the transmit nodes move within the square area $\mathcal{U}$, such that $d \le p_i(t) \le d+s$ and $-s/2 \le q_i(t) \le s/2$ for $0 \le t \le t_{\max}$. Define K *i.i.d.* Brownian motions over the complex plane with the diffusion coefficient D as $\mathbf{W}_i = \{w_i(t) = u_i(t) + \mathrm{i}v_i(t),\ 0 \le t \le t_{\max}\}$, $1 \le i \le K$, where $u_i(t+h) - u_i(t)$ and $v_i(t+h) - v_i(t)$ are independent Gaussian random variables with zero mean and variance $Dh/2$. Intuitively, the diffusion coefficient D (in squared meter per second) is the mean squared displacement of a Brownian particle over one second, i.e., $\mathbb{E}[|w_i(t+1) - w_i(t)|^2] = D$. We assume the motions of transmit nodes are modeled as *i.i.d.* Brownian motions with reflected boundaries of the area $\mathcal{U}$ as

$$p_i(t) = \begin{cases} u_i(t), & t \in \mathcal{T}_{i,1} \\ 2d - u_i(t), & t \in \mathcal{T}_{i,2}, \\ 2(d+s) - u_i(t), & t \in \mathcal{T}_{i,3} \end{cases}$$

$$q_i(t) = \begin{cases} v_i(t), & t \in \mathcal{S}_{i,1} \\ -s - v_i(t), & t \in \mathcal{S}_{i,2}. \\ s - v_i(t), & t \in \mathcal{S}_{i,3} \end{cases} \quad (4)$$

where $t \in \mathcal{T}_{i,1}$ when $d < u_i(t) < d+s$, $t \in \mathcal{T}_{i,2}$ when $u_i(t) \le d$, $t \in \mathcal{T}_{i,3}$ when $u_i(t) \ge d+s$, $t \in \mathcal{S}_{i,1}$ when $-s/2 < v_i(t) < s/2$, $t \in \mathcal{S}_{i,2}$ when $v_i(t) \le -s/2$, and $t \in \mathcal{S}_{i,3}$ when $v_i(t) \ge s/2$.

C. Transmit Node Selection

We assume that the transmit nodes can measure the path losses $\{g_k(t)\}_{1 \le k \le K}$ of their own channels and the measurements can be fed back to the transmit head node. The path-loss measurements can be taken using a similar method as in LTE, which are used for the purpose of power control between base station and users ([16]). By leveraging the knowledge of path loss $\mathbf{G}(t)$, we consider a simple and practical node selection scheme to exploit the performance of RD-MIMO with reduced operational costs. Specifically, a subset of L $(L \le K)$ nodes is activated for the cellular transmissions, which have the smallest path losses towards the receive cluster. The L active transmit nodes are assumed to track the variations of the path losses for the rate adaptation purpose. When the number of available transmit nodes is large, selecting a small subset of nodes could reduce the power consumption and signaling overheads induced by the channel measurements and feedbacks. In addition, as will be shown in Section IV, the RD-MIMO channel may achieve an optimal rate by properly selecting the number of active nodes. The node selection procedure is as follows:

(P1) Given a set of K candidate transmit nodes, which are assumed to be located in the square area $\mathcal{U}$ as shown in Fig. 1. The size of $\mathcal{U}$ is determined by the system configurations, such as the coverage area of WiFi links, node density, fading characteristics, etc.

(P2) At time t, the transmit head node triggers the channel feedback, where the path losses $\{g_k(t)\}_{1 \le k \le K}$ are sent to the transmit head node.

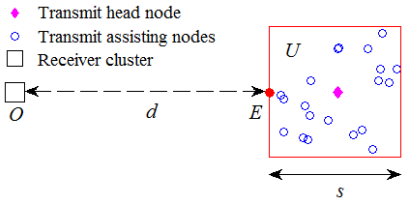

Fig. 1. RD-MIMO with two cooperative clusters with inter-cluster distance $\boldsymbol{d}$. The edge length of the square transmit cluster is $\boldsymbol{s}$.

(P3) The head node activates the L transmit nodes having the largest average channel gains, as measured in (P2), to form the transmit cluster, i.e., the active nodes have

$$g_{(1)}(t) \ge g_{(2)}(t) \ge \cdots \ge g_{(L)}(t), \quad (5)$$

where $g_{(i)}(t)$ is the i^{th} largest channel gain among $g_1(t), \ldots, g_K(t)$ at time t. The transmit power is equally allocated to the active nodes, while the inactive nodes are muted.

Due to the approximation (3) and the selection criterion (5), the receive signal $\mathbf{y}(t)$ after transmit node selection can be rewritten as

$$\mathbf{y}_{(L)}(t) = \mathbf{H}_{(L)}(t)\, \mathbf{G}_{(L)}(t)\, \mathbf{x}_{(L)}(t) + \mathbf{n}(t), \quad (6)$$

where $N \times L$ matrix $\mathbf{H}_{(L)}(t)$ denotes the fast fading between the active transmitters and the receive cluster, and $\mathbf{G}_{(L)}(t)$ is a diagonal matrix with the i^{th} diagonal entry being $g_{(i)}(t)$. The entry-wise matrix multiplication in (1) reduces to the standard matrix multiplication in (6). The Gaussian vector $\mathbf{x}_{(L)}(t)$ denotes the transmitted signal at the active nodes, such that $\mathbf{x}_{(L)}(t) \sim \mathcal{CN}(0, P/L\, \mathbf{I})$, where P is the total transmit power.

III. Performance Analysis of RD-MIMO with Transmitter Selection

In this section, the performance of the RD-MIMO system with transmitter selection is evaluated in terms of the average achievable rate. Denoting C_L as the Shannon capacity of the channel (6), the average achievable rate is defined as $\mathcal{R}_L = \mathbb{E}[C_L]$ averaged over fast fading matrix $\mathbf{H}_{(L)}(t)$ and the path loss matrix $\mathbf{G}_{(L)}(t)$. The achievable rate $\mathcal{R}_L$ has the operational meaning that the transmission rate of RD-MIMO channel (6) is expected to be $\mathcal{R}_L$ for a typical node placement inside the area $\mathcal{U}$, where the transmit nodes are independently and randomly distributed ([17]). In addition, due to the node mobility, the time interval to perform the cluster reselection is estimated, assuming the transmit nodes are modeled as Brownian particles. In this section, the subscript (L) and the time index (t) in (6) will be dropped whenever it is clear from the context.

A. Average Achievable Rate

Due to assumptions (A1)-(A3), the Shannon capacity of the channel (6) is given by [3] in nats/s/Hz as[4]

$$C_L = \frac{1}{N} \log \det\left(\mathbf{I} + \frac{\gamma}{L}\mathbf{H}\boldsymbol{\Sigma}\mathbf{H}^{\dagger}\right) = \frac{1}{N}\sum_{i=1}^{N} \log\left(1 + \frac{\gamma}{\zeta}\lambda_i\right), \quad (7)$$

[4] $\det(\cdot)$ denotes the determinant of matrix.

where $\gamma = Pg_0^2/\rho^2$ is the average received SNR if a transmitter is located at point E in Fig. 1 with the transmission power P. The $L \times L$ diagonal matrix $\mathbf{\Sigma} = 1/g_0^2\mathbf{G^2}$ with $g_0 = c_p d^{-\alpha/2}$ and the i^{th} diagonal entry being $\sigma_{(i)} = (g_{(i)}/g_0)^\alpha = (d/d_{(i)})^\alpha$. The second equality of (7) is obtained by the eigenvalue decomposition, where λ_i, $1 \le i \le N$, are the eigenvalues of $\mathbf{H\Sigma H}^\dagger/N$ and $\zeta = L/N$.

To gain insights into the rate $\mathcal{R}_L$, we adopt an asymptotic spectral analysis of the large random matrix $\mathbf{H\Sigma H}^\dagger/N$. In the following, we consider the asymptotic regime

$$L, N \to \infty, \quad \text{with} \quad 0 < \zeta = \frac{L}{N} < \infty. \tag{8}$$

In the regime (8), the asymptotic $\mathcal{R}_L$ is given in the following proposition, assuming integer value of path-loss exponent α.

Proposition 1 *In the asymptotic regime (8) with integer values of α, the average achievable rate $\mathcal{R}_L = \mathbb{E}[C_L]$ almost surely converges to a nonrandom limit as:*

$$\mathcal{R}_L \overset{(8)}{\to} \zeta\, \mathcal{V}\left(\frac{\eta\gamma}{\zeta}\right) + \log\frac{1}{\eta} + \eta - 1, \tag{9}$$

where $\eta \ge 0$ is the solution of the fixed-point equation

$$\zeta = \frac{1-\eta}{1-\frac{\zeta}{\gamma\eta}\mathcal{G}\left(-\frac{\zeta}{\gamma\eta}\right)}. \tag{10}$$

The functions $\mathcal{V}(\gamma)$ and $\mathcal{G}(\omega)$ are given by

$$\mathcal{V}(\gamma) = \frac{1}{\alpha}\sum_{i=1}^{\alpha}\int_0^\gamma \frac{x^{\frac{1}{\alpha}-1}}{x^{\frac{1}{\alpha}} - e^{\frac{2i+1}{\alpha}\pi\mathrm{i}}} \times_3 F_2\left(1,1,L+1;2,K+1;\frac{1}{\theta(x^{\frac{1}{\alpha}}e^{-\frac{2i+1}{\alpha}\pi\mathrm{i}}-1)}\right)\mathrm{d}x, \tag{11}$$

$$\mathcal{G}(\omega) = \frac{1}{\alpha\,\omega}\sum_{i=1}^{\alpha}\frac{1}{1-|\omega|^{\frac{1}{\alpha}}e^{\frac{2i+1}{\alpha}\pi\mathrm{i}}} \times_3 F_2\left(1,1,L+1;2,K+1;\frac{1}{\theta(|\omega|^{-\frac{1}{\alpha}}e^{-\frac{2i+1}{\alpha}\pi\mathrm{i}}-1)}\right) - \frac{1}{\omega}, \tag{12}$$

where $\theta = d/s$ and ${}_3F_2$ denotes the generalized hypergeometric function [[18], Eq. (9.14.1)].

Proof. The proof of Proposition 1 is a direct application of [[19], Th. 2.39] using the spectral distribution of $\mathbf{\Sigma}$. We omit the proof due to page limitation.

Numerical results in Section IV show that the asymptotic rate in Proposition 1 can serve as good approximations for practical RD-MIMO systems with "not-so-large" L and N. We note that the intermediate result [[19], Th. 2.39] was originally used to calculate the asymptotic capacity of the C-MIMO channels in presence of spatial correlations, where $\mathbf{\Sigma}$ is the correlation matrix among the transmit antennas. Results therein depend on the empirical distribution of the entries of $\mathbf{\Sigma}$. On the other hand, Proposition 1 is obtained by averaging over the node distribution law within the cluster area $\mathcal{U}$, which requires non-trivial follow-up derivations from [[19], Th. 2.39].

B. Node Reselection Time

As the transmit nodes move randomly, the subset of the transmit nodes with top channel gains changes over time. When some inactive nodes experience more favorable channels compared to the active nodes, reselection of a new transmit cluster is needed to fully utilize the performance of RD-MIMO. However, as assumed in Section II-C, the path losses are tracked by the active transmitters only. To timely capture the reselection event, the transmit head node periodically triggers the channel measurements and feedbacks from all candidate transmit nodes to the head node. The frequency of the cluster reselection needs to be properly set to achieve a tradeoff between the performance and the operational costs.

For a fixed ε $(0 < \varepsilon < 1)$, the node reselection time t_ε is set to capture $(1-\varepsilon)$-percent of the reselection events due to the node mobility. Denote τ as the time interval between consecutive cluster reconfiguration events as defined below in (14) and let $H(t)$ to be the distribution of τ assuming Brownian motion model. The reselection time t_ε is set as to satisfy

$$\varepsilon = \Pr(\tau < t_\varepsilon) = H(t_\varepsilon), \tag{13}$$

By decreasing ε, the rate of the cluster reselections is increased, requiring more frequent channel measurements and feedbacks from the inactive transmit nodes.

Next, we give a definition of the node reselection event in term of the first hitting time between the active and inactive subsets of nodes, conditioned on initial (non-hitting) node locations. Without loss of generality, the initial distance between the receive cluster and the transmit nodes are ordered as $|a_1(0)| \le \cdots \le |a_K(0)|$, where the nodes with the index $1, \ldots, L$ correspond to the active nodes at time $t = 0$. To enable a tractable analysis, we adopt a heuristic assumption that when $d \gg s$, the distances $|a_i(t)| \approx p_i(t)$, where $p_i(t)$ is given in (4). Due to the criterion (5), the node reselection needs to be performed when any of the active node has larger distance towards the receive cluster, compared to any of the inactive node. Given the initial (non-hitting) node locations, the time instance to perform a cluster reselection is defined as

$$\tau = \inf\left\{t \ge 0: \max_{1\le i\le L} p_i(t) \ge \min_{L+1\le i\le K} p_i(t)\right\}. \tag{14}$$

In addition, we define the pairwise hitting time between the transmit nodes i and j, $1 \le i \le L$ and $L+1 \le j \le K$, as $\tau_{i,j} = \inf\{t \ge 0: p_i(t) > p_j(t)\}$. The reselection time τ can be rewritten in terms of $\tau_{i,j}$ as $\tau = \min_{i,j}(\tau_{i,j})$ and the distribution of τ is given by $H(t) = \Pr(\tau < t) = 1 - \Pr(\min_{i,j}(\tau_{i,j}) > t)$. Using the Fréchet's inequality ([20]), $H(t)$ is lower-bounded as

$$H(t) \ge \max_{i,j} \Pr(\tau_{i,j} < t) = \max_{i,j} H_{i,j}(t) = H_L(t), \tag{15}$$

where $H_{i,j}(t)$ is the first hitting time distribution of the nodes i and j, and we denote $H_L(t) \equiv H_{L,L+1}(t)$ for simplicity. The third equality in (15) is clear, since $H_L(t)$ is the first hitting time distribution between two nearest nodes from the active and inactive sets. Assume at time $t = 0$ the system completes the previous node selection and the node motions are in the steady state[5], such that the position of an arbitrary node is uniformly distributed within the square area $\mathcal{U}$. Based on these assumptions, an approximation for the first hitting time distribution $H_L(t)$ is given by the following proposition.

[5] In practical system, when the system detects a hitting event defined in (14), there exists operational latency to perform the actual node reselection procedures. When the latency is large, the node motions are assumed to be in the steady state.

Proposition 2 *The first hitting time distribution* $H_L(t) = Pr(\tau_{L,L+1} < t)$ *is approximated by*

$$H_L(t) \approx e^{\frac{c_1^2}{8c_2}} \sum_{n=0}^{K-1} (-1)^n \mathcal{D}_n \cdot (K-n)_{n+1} \left(\frac{2Dt}{s^2 c_2}\right)^{\frac{n+1}{2}}, \quad (16)$$

where $(a)_m = a(a+1)\cdots(a+m)$ *denotes the Pochhammer symbol, the constants* $c_1 = 1.095$ *and* $c_2 = 0.7565$, $\mathcal{D}_n = D_{-n-1}\left(c_1/\sqrt{2c_2}\right)$, *and* $D_{(\cdot)}(\cdot)$ *denotes the parabolic cylinder function [[18], Eq. (9.240)].*

Proof. The proof of Proposition 2 starts by establishing the equivalence between a pair of one-dimensional Brownian motions and a single two-dimensional Brownian motion similar to [21]. The first hitting time distribution is then obtained by using [0, Eq. (X.5.8)] and applying non-linear least square approximation to the Gaussian distribution. The detail of the proof is omitted due to page limitation.

Using Proposition 2, the reselection time t_ε, defined in (15), can be estimated as $t_\varepsilon = H^{-1}(\varepsilon) \le H_L^{-1}(\varepsilon)$ by solving the inverse function of $H_L(\cdot)$. In addition, numerical results show that the finite summation (16) can be further approximated by taking the first two summands with $n = 0$ and $n = 1$ for a wide range of system settings. This reduces $H_L(t)$ to a quadratic function in $\sqrt{t}$, and the reselection time t_ε can be explicitly solved as

$$t_\varepsilon \approx \frac{s^2 c_2 K^{-1} \mathcal{D}_1^{-2}}{4D(K-1)^2} \left(K\mathcal{D}_0^2 - 2(K-1)\mathcal{D}_1 e^{-\frac{c_1^2}{8c_2}\varepsilon} - \mathcal{D}_0 \sqrt{K^2\mathcal{D}_0^2 - 4K(K-1)\mathcal{D}_1 e^{-\frac{c_1^2}{8c_2}\varepsilon}} \right). \quad (17)$$

As the number of nodes K increases, it is clear from (17) that $t_\varepsilon \sim \mathcal{O}(1/K^2)$ for a fixed probability ε. Using the well-known opportunistic channel feedback, the amount of feedback scales as $\log(K)$. Thus, overall, the computational complexity (number of channel measurements to be processed per unit time) at the transmit head node scales as $\mathcal{O}(K^2 \log K)$. When K is large, the computational complexity may be prohibitively large and a node pre-selection is needed to randomly choose a subset of the K nodes to be the candidates in the follow-up node selection. In the pre-selection phase, each node independently and locally decides whether to participate in the cluster (re-)configuration, and thus, reducing the feedback overhead of the system.

IV. Numerical Results

First, we investigate the impacts of the number of active nodes on the achievable rate in the large and small SNR regimes. Assuming the number of receive nodes is fixed to be $N = 8$, the number of candidate transmit nodes is set to be $K = 10, 20, 40,$ and 60, which are uniformly distributed in the square area $\mathcal{U}$ with $s = 15$ meters. The distance between the transmit and receive clusters is $d = 30$ meters with path-loss exponent $\alpha = 4$. Fig. 2(a) shows the average achievable rate $\mathcal{R}_L$ as a function of the percentage of active transmit nodes L/K, when SNR $\gamma = 10$ dB. For a given number of candidate transmit nodes K, there exists an optimal number of active transmit node L that maximizes the average achievable rate of the RD-MIMO transmission, e.g., 9-18 active nodes among 10-60 candidate nodes should be used for optimal rate. The transmit node selection scheme is more effective in the low SNR regime with $\gamma = -10$ dB, as shown in Fig. 2(b), where only 3-6 best nodes are needed to maximize the achievable rate. These results confirm the importance of selecting a few best nodes in the RD-MIMO communication scenario.

In the following simulations, we show the impact of the number of transmit nodes on the cluster reconfiguration time, and we use the reselection time (17) obtained for the Brownian motion model to estimate the reselection time for the random walk mobility model. In the cases of the random walk, the walk step per unit time δ_t is set to $\triangle_a = 0.05$ meters with the instantaneous velocities of $v_{\text{node}} = \triangle_a/\delta_t = 1, 5,$ and 10 meters/second (which correspond to 3.6 km/h, 18 km/h, and 36 km/h, respectively). Accordingly, the diffusion coefficient D is set such that the mean square displacements of the Brownian motion and the random walk are equal in each step, i.e., $D\,\delta_t = \triangle_a^2$. Fig. 3 shows the reselection time t_ε with $\varepsilon = 20\%$ as a function of the number of available nodes K in the cluster area $\mathcal{U}$. The number of active nodes is set to $L = 4$, the inter-cluster distance is $d = 50$ meters, and the edge length of the transmit cluster is $s = 5$ meters. At low velocity of $v_{\text{node}} = 1$, the reselection needs to be performed within 3000 milliseconds when the number of available nodes is small. As K increases, the required reselection time decreases to hundreds of milliseconds. In the case of larger velocities with $v_{\text{node}} = 5$ and 10, the reselection time is between 10 to 100 milliseconds for most of the considered values of K, which is feasible in practical cellular systems, such as in LTE ([16]), where the radio resource granularity in time domain is 1 millisecond. In all cases, the analytical expression (17) provides a useful estimate for the order of magnitude of the reselection time of the corresponding random walk models.

V. Conclusions

We consider the RD-MIMO architecture with the antenna arrays formed by the mobile user devices. In the considered system, the communicating devices temporarily recruit cluster of cooperative nodes, where the cluster cooperation is via large data rate local wireless connections. We present the analytical framework to quantify the performance of the RD-MIMO system and evaluate the time scale of the cluster reconfiguration due to the node mobility. Our findings suggest that the achievable rate of the RD-MIMO system can be maximized by optimally selecting a subset of the available transmit nodes depending on their large-scale fading. The cluster reconfiguration to select a new set of transmit nodes with favorable channel conditions is shown to be highly affected by the number of transmit nodes K. As K increases, the time interval between reconfigurations decreases and the incurred computational complexity scales as $\mathcal{O}(K^2 \log K)$. The simulation results show that the reconfiguration time, obtained for the Brownian motion model, provides an estimate for the order of magnitude of the corresponding random walk models.

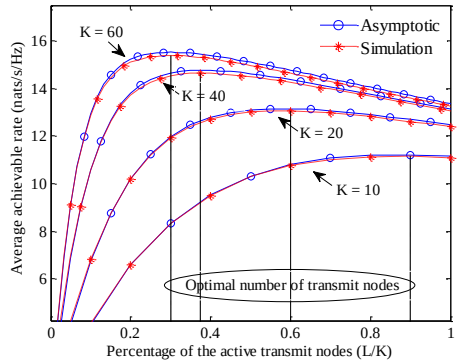

(a)

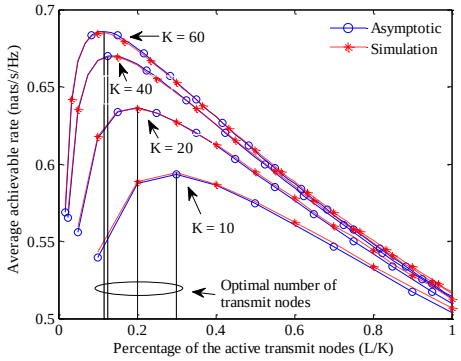

(b)

Fig. 2. Average achievable rate of RD-MIMO with transmit node selection. The number of receive nodes is $N = 8$. Lines labeled with "$\circ$" denote average rates obtained by (9), lines labeled with "$*$" denote simulation results, and dashed vertical lines denote the optimal percentage of active transmit nodes. (a) SNR $\gamma = 10$dB, (b) SNR $\gamma = -10$dB.

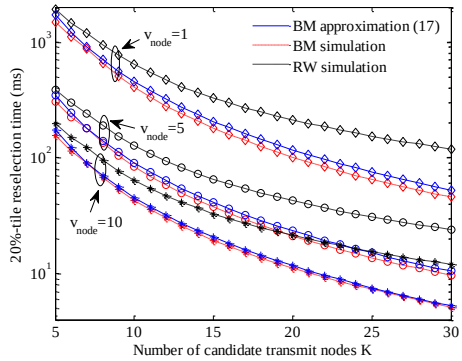

Fig. 3. Comparison of 20%-tile reselection time between Brownian Motion (BM) and Random Walk (RW) models. The walk step of RW is $\Delta_a = 0.05$ meters with various walk speeds $v_{\text{node}} = \Delta_a/\delta_t$. The diffusion coefficient D is set as $D = \Delta_a^2/\delta_t = \Delta_a \cdot v_{\text{node}}$. The number of active transmit nodes is fixed to be $L = 4$.

REFERENCES

[1] J. N. Laneman and G. W. Wornell, "Distributed space-time-coded protocols for exploiting cooperative diversity in wireless networks," *IEEE Trans. Inf. Theory*, vol. 49, no. 10, pp. 2415–2425, Oct. 2003.

[2] A. Abdi and M. Kaveh, "A space-time correlation model for multielement antenna systems in mobile fading channels," *IEEE J. Sel. Areas Commun.*, vol. 20, no. 3, pp. 550–560, Apr. 2002.

[3] D. Aktas, M. N. Bacha, J. S. Evans, and S. V. Hanly, "Scaling results on the sum capacity of cellular networks with MIMO links," *IEEE Trans. Inf. Theory*, vol. 52, no. 7, pp. 3264–3274, July 2006.

[4] W. Roh and A. Paulraj, "MIMO channel capacity for the distributed antenna systems," in *Proc. IEEE Veh. Technol. Conf.*, Sept. 2002, pp. 706–709.

[5] H. Hub, A. M. Tulino, and G. Caire, "Network MIMO with linear zero-forcing beamforming: Large system analysis, impact of channel estimation, and reduced-complexity scheduling," *IEEE Trans. Inf. Theory*, vol. 58, no. 5, pp. 2911-2934, May 2012.

[6] C. Zhong, K.-K. Wong, and S. Jin, "Capacity bounds for MIMO Nakagami-m fading channels," *IEEE Trans. Signal Process.*, vol. 57, no. 9, pp. 3613–3623, Sept. 2009.

[7] M. Matthaiou, N. D. Chatzidiamantis, and G. K. Karagiannidis, "A new lower bound on the ergodic capacity of distributed MIMO systems," *IEEE Signal Process. Lett.*, vol. 18, no. 4, pp. 227–230, Apr. 2011.

[8] M. Chiani, M. Z. Win, and H. Shin, "MIMO networks: The effects of interference," *IEEE Trans. Inf. Theory*, vol. 56, no. 1, pp. 336–349, Jan. 2010.

[9] O. Simeone, O. Somekh, H. V. Poor, and S. Shamai, "Distributed MIMO systems for nomadic applications over a symmetric interference channel," *IEEE Trans. Inf. Theory*, vol. 55, no. 12, pp. 5558–5574, Dec. 2009.

[10] S. Cui, A. Goldsmith, and A. Bahai, "Energy-efficiency of MIMO and cooperative MIMO techniques in sensor networks," *IEEE J. Sel. Areas Commun.*, vol. 22, no. 6, pp. 1089-1098, Aug. 2004.

[11] S. K. Jayaweera, "Virtual MIMO-based cooperative communication for energy-constrained wireless sensor networks," *IEEE Trans. Wireless Commun.*, vol. 5, no. 5, pp. 984-989, May 2006.

[12] D. N. Nguyen and M. Krunz, "A cooperative clustering protocol for energy constrained networks," in *Proc. SECON*, Salt Lake City, UT, June 2011, pp. 574-582.

[13] W. Saad, Z. Han, M. Debbah, and A. Hjørungnes, "A distributed coalition formation framework for fair user cooperation in wireless networks," *IEEE Trans. Wireless Commun.*, vol. 8, no. 9, pp. 4580-4593, Sept. 2009.

[14] S. H. Lee, D. R. Shin, H. W. Jeong, and Y. H. Kim, "Distributed bargaining strategy for downlink virtual MIMO with device-to-device communication," *IEEE Trans. Commun.*, vol. 64, no. 4, pp. 1503-1516, Apr. 2016.

[15] M. Webb, M. Yu, and M. Beach, "Propagation characteristics, metrics, and statistics for virtual MIMO performance in a measured outdoor cell," *IEEE Trans. Antennas Propag.*, vol. 59, no. 1, pp. 236-244, Jan. 2011.

[16] TS 36.213 V13.2.0, Tech. Spec. Group Radio Access Network, Evolved Universal Terrestrial Radio Access (E-UTRA); Physical Layer Procedures (Release 13), 2016.

[17] J. G. Andrews, F. Baccelli, and R. K. Ganti, "A tractable approach to coverage and rate in cellular networks," *IEEE Trans. Commun.*, vol. 59, no. 11, pp. 3122-3134, Nov. 2011.

[18] I. S. Gradshteyn and I. M. Ryzhik. *Table of Integrals, Series, and Products*, 7th ed. New York: Academic Press, 2007.

[19] A. M. Tulino and S. Verdú. *Random Matrix Theory and Wireless Communications*. now Publishers, 2004.

[20] T. Hailperin. *Boole's Logic and Probability*, 2nd ed. North Holland: Elsevier, 1986.

[21] R. Groenevelt, E. Altman, and P. Nain, "Relaying in mobile ad hoc networks: The Brownian motion mobility model," *Wireless Netw.*, vol. 12, no. 5, pp. 561–571, Sept. 2006.

[22] W. Feller. *An Introduction to Probability Theory and Its Applications*, 2nd ed. New York: John Wiley & Sons, 1971.